Check for updates

Interleukin-23 acts as antitumor agent on childhood B-acute lymphoblastic leukemia cells

Claudia Cocco,[1] Sara Canale,[1] Chiara Frasson,[2] Emma Di Carlo,[3] Emanuela Ognio,[4] Domenico Ribatti,[5] Ignazia Prigione,[6] Giuseppe Basso,[2] and Irma Airoldi[1]

[1]Associazione Italiana per la Ricerca sul Cancro (AIRC) Laboratory of Immunology and Tumors, Department of Experimental and Laboratory Medicine, G. Gaslini Institute, Genova, Italy; [2]Division of Hematology Oncology, Department of Pediatrics, University of Padova, Padova, Italy; [3]Department of Oncology and Neurosciences, G. d'Annunzio University and Centro delle Scienze dell'Invecchiamento Aging Research Center, G. d'Annunzio University Foundation, Chieti, Italy; [4]Animal Model Facility, Istituto Nazionale per la Ricerca sul Cancro, Genova, Italy; [5]Department of Human Anatomy and Histology, University of Bari, Bari, Italy; and [6]Laboratory of Oncology, G. Gaslini Institute, Genova, Italy

Interleukin (IL)–23 is a proinflammatory cytokine belonging to the IL-12 superfamily. The antitumor activity of IL-23 is controversial, and it is unknown whether or not the cytokine can act directly on tumor cells. The aim of this study was to investigate the potential direct antitumor activity of IL-23 in pediatric B-acute lymphoblastic leukemia (B-ALL) cells and to unravel the molecular mechanisms involved. Here, we show, for the first time, that IL-23R is up-regulated in primary B-ALL cells, compared with normal early B lymphocytes, and that IL-23 dampens directly tumor growth in vitro and in vivo through the inhibition of tumor cell proliferation and induction of apoptosis. The latter finding is related to IL-23–induced up-regulation of miR15a expression and the consequent down-regulation of BCL-2 protein expression in pediatric B-ALL cells. This study demonstrates that IL-23 possesses antileukemic activity and unravels the underlying mechanisms. Thus, IL-23 may be a candidate novel drug for the treatment of B-ALL patients unresponsive to current therapeutic standards. (*Blood*. 2010;116(19):3887-3898)

Introduction

Interleukin (IL)–23 is a heterodimeric cytokine composed of the promiscuous IL-12p40 and the exclusive p19 subunits.[1] The IL-23 receptor (IL-23R) is composed of the IL-12Rβ1 chain and the unique IL-23R chain that are associated with Jak2 and STAT3.[2] In T lymphocytes and leukemic T cells, IL-23 induces activation of STAT family members (ie, STAT1, 3, 4, and STAT5).[2] IL-23 is produced predominantly by myeloid dendritic cells (DCs) activated by Toll-like receptor (TLR)–2, -4, and -8 ligands[3-5] and by type 1 macrophages.[6] This cytokine is now considered the master switch in several T cell–mediated inflammatory disorders,[7-10] such as experimental autoimmune encephalomyelitis, inflammatory bowel disease, psoriasis, and *Helicobacter pylori*–associated gastritis. The antitumor activity of IL-23 is controversial. It has been shown that proinflammatory cytokines, including IL-17A, IL-6, and IL-23, can impair $CD8^+$ T cell–mediated immune surveillance and promote de novo carcinogenesis and tumor neovascularization via STAT3 signaling and additional mechanisms.[11-15] In contrast, other groups have shown that IL-23 exerts antitumor activity through the stimulation of T and natural killer (NK) cells.[16-23] So far, no information is available on the direct activity of this cytokine on tumor cells.

MicroRNA are small noncoding RNA with regulatory function implicated in human tumorigenesis,[24-31] since the main target mRNA transcripts are involved in proliferation, apoptosis, and differentiation. Moreover, recent studies demonstrated that reduced mature microRNA expression can promote tumorigenesis.[32,33] In this study, we investigated the expression and function of IL-23R in pediatric B-acute lymphoblastic leukemia (B-ALL) cells and in their normal counterparts and the potential IL-23 antitumor activity against B-ALL cells in vitro and in vivo, unraveling the mechanisms involved and focusing on the ability of IL-23 to modulate microRNA expression.

Methods

Patient samples

Bone marrow (BM) aspirates from 4 pro-B, 19 early pre-B, and 6 pre-B pediatric ALL patients were performed for diagnostic purposes at disease onset after informed consent from children's parents or their legal guardians. The main demographic, immunologic, and cytogenetic features of the patients are shown in Table 1. Aliquots of BM aspirates performed for diagnostic purposes from 12 age-matched individuals not affected by oncologic disorders were obtained after informed consent. The study design was approved by the Ethical Committee of the University of Padova, Padova, Italy, and conformed with the principles of the Declaration of Helsinki. Mononuclear cell suspensions of leukemic and normal BM cells were isolated on Ficoll-Hypaque density gradients and frozen in liquid nitrogen. Leukemic B cells were purified by positive selection of $CD19^+$ cells using magnetic beads (Miltenyi Biotec), according to the manufacturer's instructions.

Immunophenotypic characterization of B-ALL cells was carried out as previously described.[34] Normal pro-B, early pre-, and pre-B cells were identified as $CD19^+CD10^+CD20^-$, $CD19^+CD10^+CD20^+$, or $CD19^+CD10^-CD20^+$ cell fractions, respectively.

Cell culture, reagents, and antibodies for flow cytometry

The human RS4;11 pro-B ALL cell line, and the Nalm-6 and 697 pre-B ALL cell lines were cultured in RPMI 1640 medium with 10% fetal calf serum (FCS; Seromed-Biochrom KG). Human recombinant (hr)IL-23 and

Submitted October 13, 2009; accepted July 18, 2010. Prepublished online as *Blood* First Edition paper, July 29, 2010; DOI 10.1182/blood-2009-10-248245.

The publication costs of this article were defrayed in part by page charge payment. Therefore, and solely to indicate this fact, this article is hereby marked "advertisement" in accordance with 18 USC section 1734.

© 2010 by The American Society of Hematology

Downloaded from http://ashpublications.net/blood/article-pdf/116/19/3887/1490759/zh804510003887.pdf by guest on 02 June 2024

Table 1. Clinical and laboratory features of B-ALL patients

Patient no.	Sex	Age, y	Immunologic subtype	Genetic translocation
1	F	7	Early-pre	9;22/4;11 neg*
2	F	6	Early-pre	9;22/4;11 neg
3	F	5	Early-pre	9;22/4;11 neg
4	F	4	Early-pre	9;22/4;11 neg
5	M	3	Early-pre	9;22/4;11 neg
6	M	2	Early-pre	9;22/4;11 neg
7	F	8	Early-pre	12;21
8	F	7	Early-pre	12;21
9	M	6	Early-pre	12;21
10	M	5	Early-pre	Neg†
11	M	3	Early-pre	12;21
12	M	2	Early-pre	9;22 and 1;19
13	M	6	Early-pre	12;21
14	M	2	Early-pre	Neg
15	M	8	Early-pre	Neg
16	M	5	Early-pre	Neg
17	M	4	Early-pre	Neg
18	M	12	Early-pre	Neg
19	F	6	Early-pre	Neg
20	M	6	Pre-B	12;21
21	M	3	Pre-B	Neg
22	M	2	Pre-B	Down syndrome
23	F	8	Pre-B	1;19
24	F	8	Pre-B	Neg
25	M	6	Pre-B	Neg
26	F	< 1 (infant)	Pro-B	4;11
27	F	3	Pro-B	Neg
28	F	5	Pro-B	Neg
29	M	4	Pro-B	4;11

All data are as of diagnosis. The following genetic translocations have been tested: 9;22, 4;11, 12;21, and 1;19.
*9;22/4;11 neg indicates these patients did not show 9;22 or 4;11 translocations. Other translocations have not been tested.
†Neg indicates negative. These patients did not show any genetic translocation.

goat immunoglobulin (Ig)G anti–human IL-23R were from R&D Systems. The concentrations of IL-23 tested in vitro ranged from 10 to 200 ng/mL. Fluorochrome-conjugated anti-BCL2 and -Ki67 monoclonal antibodies (mAbs) were from Dako. Fluorochrome-conjugated CD10, CD19, CD20, and anti–phospho-STAT4 mAbs were from BD Biosciences. Phycoerythrin (PE)–conjugated Ig swine anti–goat and nonimmune goat IgG were from Caltag. Cells were scored by FACSCalibur analyzer (BD Biosciences), and data were processed using CellQuest software Version 3.3 (BD Biosciences).

Western blot

IL-23 signal transduction was studied in 697 cells starved 4 hours in serum-free medium and cultured for an additional 30 minutes with or without interferon (IFN)-α (positive control, 1000 U/mL; Sigma-Aldrich) or IL-23 (100 ng/mL). BCL-2 expression and poly(ADP-ribose)polymerase (PARP) cleavage were analyzed in 697 cells treated or not with IL-23 (24 and 48 hours). Total protein was extracted from 10^7 cells using Cell Extraction Buffer (Invitrogen) with a protease-inhibitor cocktail (Sigma-Aldrich). Proteins were quantified with the Pierce BCA Protein Assay kit (Thermo Scientific). Proteins (20 μg) were loaded on 12% polyacrylamide gel, transferred to nitrocellulose membrane (Hybond-C Extra; Amersham Biosciences), and stained with antiphosphorylated or -unphosphorylated STAT antibodies (Phospho-STAT and STAT Antibody Sampler kits; Cell Signaling Technology), anti–BCL-2, anti–cleaved PARP (also used by flow cytometry), and anti–phospho-STAT4 antibodies (Zymed). Anti–BCL-2 or PARP antibodies were used in association with anti-GAPDH (glyceraldehyde-3-phosphate dehydrogenase) antibody (Ab; Cell Detection kit; Amersham).

Cell-proliferation and apoptosis assays

Five primary B-ALL cell fractions and the 697 cells were cultured 6, 24, and 48 hours with or without 100 ng/mL hrIL-23, after titration experiments. Cells were stained with anti-Ki67 or anti-BCL-2 mAb (cytofix/cytoperm kit; BD Biosciences) and analyzed by flow cytometry. Apoptosis was assessed using the annexin V/fluorescein isothiocyanate (FITC) kit (Bender MedSystems). In some experiments, 2 primary B-ALL samples and the 697 cells were cultured 30 minutes with or without 100 ng/mL IL-23 and analyzed for AKT, p38MAPK (mitogen-activated protein kinase), and extracellular signal-regulated protein kinase (ERK)1/2 phosphorylation (Cell Signaling Technology). In the latter experiments, positive control was the Jurkat cell line stimulated 30 minutes with phorbol myristate acetate (PMA; 20 ng/mL; Sigma-Aldrich), according to the manufacturer's protocol. The same B-ALL samples were cultured 24 and 48 hours with or without IL-23 and tested for caspase-3, -7, -8, and -10 activation using the ApoFluor Green Caspase activity kit (ICN Biomedicals). In these experiments, positive control was the U266 cell line stimulated 24-48 hours with 10nM bortezomib (Sigma-Aldrich). In another set of experiments, the 697 cells were pretreated 1 hour with the N-Benzyloxycarbonyl-Val-Ala-Asp(O-Me) fluoromethylketone (Z-VAD-FMK) pancaspase inhibitor (100μM; Sigma-Aldrich), cultured with IL-23 for an additional 24-48 hours, and tested for apoptosis by flow cytometry. Cell-cycle analysis was performed as previously described[35] on 697 cells cultured with or without IL-23 (24-48 hours) or after stimulation for 24, 48, 72, and 96 hours with the following: anti–human CD40 (100 ng/mL; ImmunoTools), CpG 2395 (4 μg/mL; Coley Pharmaceutical), and anti–human IgA-G-M, H+L chains (2 μg/mL; Jackson ImmunoResearch Laboratories).

CAM assay

Chorioallantoic membrane (CAM) assay was performed as previously reported.[36] Sponges were loaded with the following: 1 μL of phosphate-buffered saline (PBS; negative control); 1 μL of PBS with 250 ng of vascular endothelial growth factor (VEGF; R&D Systems, positive

Downloaded from http://ashpublications.net/blood/article-pdf/116/19/3887/1490759/zh804510003887.pdf by guest on 02 June 2024

control); 1 μL of medium from 697 cells and from primary B-ALL cells cultured 48 hours with or without IL-23 (100 ng/mL); or 1 μL of medium containing 100 ng/mL IL-23.

Silencing of microRNA (miR)15a and IL-23R

Silencing of miR15a in the 697 cells and in 5 primary early pre-B samples was achieved by transfection with siPORT NeoFX solution plus 100μM anti-miR15a or irrelevant anti-miR (negative control; reagents from Ambion). The 697 cells were silenced for IL-23R expression by Silencer select predesigned *si*-RNA (Ambion), according to the manufacturer's protocol.

Overexpression of miR15a

The Nalm-6 cells were stably transfected with pEP-hsa-miR15a or pEP-miR-null vector by electroporation. Briefly, 10^7 cells were suspended in 400 μL of medium and pulsed by an Electro Cell Manipulator (BTX Instrument Division; Harvard Apparatus) in the following conditions: low voltage, 1050 μF capacitance, 260 V voltage, and 30-ms pulse length. Next, cells were cultured in antibiotic-free medium for 48 hours and then for an additional 7 days with puromycin (0.5 μg/mL; Invitrogen). The 697 cells were induced to overexpress miR-15a using siPORT NeoFX solution plus 100μM hsa-miR15a precursor or irrelevant miR precursor (negative control; reagents from Ambion). miR15a expression was tested by quantitative polymerase chain reaction (PCR) in transfected cells.

Real-time PCR and miR PCR array

Twenty-nine primary B-ALL samples and 4 $CD19^+$ cell samples from normal BM were studied for IL-23R expression by quantitative PCR, as previously reported.[37] Real-time PCR was performed using human GAPDH and IL-23R primers from SABiosciences (proprietary primers, sequence not disclosed), following the experimental conditions suggested by the manufacturer.

MiR were extracted by quantitative real-time reverse transcription PCR-grade miRNA Isolation kit (SABiosciences), reverse-transcribed by a real-time reverse transcription miRNA First Strand kit (SABiosciences), and subjected to real-time PCR (Human Cancer MiRNA RT2 Profiler PCRArray; SABiosciences) as previously described.[37] The MiR PCR Array assays were performed on mature miR extracted from 6 B-ALL cell samples cultured 24 hours with or without IL-23 and from tumors explanted from hrIL-23– and PBS-treated mice injected with the 697 cells. MiR15a expression was tested by quantitative PCR in the following: (1) 697 cells cultured 48 hours with or without IL-23, (2) 697 cells transfected with anti-miR15a or irrelevant anti-miR and cultured 48 hours with or without IL-23, (3) 697 cells transfected with hsa-miR15a precursor or irrelevant miR precursor, (4) tumors from IL-23– and PBS-treated animals injected with wild-type 697 cells and transfected 697 cells with anti-miR15a or irrelevant anti-miR, (5) tumors from PBS-treated mice injected with 697 cells transfected with hsa-miR15a precursor or irrelevant miR precursor, and (6) wild-type Nalm-6 cells and transfected Nalm-6 cells with pEP-has–miR15a or p-EP–miR-null. Real-time PCR was performed using human U6 and miR15a primers from SABiosciences (proprietary primers, sequence not disclosed), following the experimental conditions suggested by the manufacturer. Relative quantification of miR15a was calculated by the $2^{-(\Delta\Delta Ct)} \pm$ SD) method.

Mouse studies

Four- to 6-week-old severe combined immunodeficient–nonobese diabetic (SCID/NOD) mice (Harlan Laboratories) were housed under specific pathogen–free conditions. All procedures involving animals were performed in the respect of the national and international regulations (D.l.vo 27/01/1992, n.116, European Economic Community Council Directive 86/609, OJL 358, December 1, 1987).

All in vivo experiments were performed using the following schedule: mice were treated intravenously with PBS or hrIL-23 (1 μg/mouse per dose) with 3 weekly doses starting 8 hours after tumor cell inoculation.

First, 2 groups of 10 animals each were injected intravenously with 5×10^6 697 cells. One group of mice was treated intravenously with hrIL-23, the other group with PBS.

Next, groups of 5 mice each were injected intravenously with 5×10^6 of the following: (1) 697 cells and treated with PBS, (2) 697 cells and treated with hrIL-23, (3) 697 cells transfected with anti-miR15a or hsa-miR15a precursor or irrelevant miR precursor and treated with PBS, (4) 697 cells transfected with anti-miR15a and treated with hrIL-23, and (5) 697 cells transfected with irrelevant anti-miR and treated with hrIL-23. Transfected cells were injected into SCID/NOD mice 24 hours after transfection. Fourteen days after tumor cell inoculation, mice were killed when signs of poor health became evident, autopsies were carried out, and tumor masses were measured.[38]

Tumorigenicity of RS4;11 and Nalm-6 cells was tested by subcutaneous (s.c.), intraperitoneum and intravenous injection using 5-10 $\times 10^6$ cells. Finally, 4 groups of 5 mice each were injected intravenously with 5×10^6 of the following: (1) Nalm-6 cells and treated with PBS, (2) Nalm-6 cells and treated with hrIL-23, (3) Nalm-6 cells transfected with pEP-hsa-miR15a and treated with PBS, and (4) Nalm-6 cells transfected with pEP-miR-null and treated with PBS. Mice were killed 5 weeks later when signs of poor health became evident. The Nalm-6 cells were searched in the peripheral blood (PB) collected from the retro-orbital sinus, in BM obtained from flushing femoral bones and in the spleen from all animals. Nalm-6 cells were identified as human $CD10^+/CD19^+$ cells.

Morphologic and immunohistochemical analyses

Tissue samples were fixed in 4% neutral buffered formalin, embedded in paraffin, sectioned at 4 μm, and stained with hematoxylin and eosin (H&E). For immunohistochemistry, paraffin-embedded sections were immunostained with anti-PCNA (Dako), anti-Cyclin D1 (Thermo Fisher Scientific), and anti-CD31 (BD Biosciences) antibodies. DNA fragmentation associated with apoptosis was detected by TUNEL staining with the ApopTag Plus Peroxidase In Situ Apoptosis kit (Millipore). Microvessels were counted in 8 randomly chosen fields under a microscope 400× field (40× objective and 10× ocular lens; 0.180 mm^2/field). The rates of proliferating cells and of apoptotic cells were determined by counting the number of positive cells/number of total cells in the viable neoplastic tissue under a microscope 600× field (60× objective and 10× ocular lens; 0.120 mm^2/field). Histologic and immunohistochemical analyses were performed under a Zeiss LSM 510 meta laser scanning confocal microscope.

Statistical analysis

Results were calculated with a 99% confidence interval. Differences in tumor volume were evaluated by the Mann-Whitney U test. Quantitative studies of stained sections were performed independently by 2 pathologists in a blind fashion. Differences in the number of proliferating cell nuclear antigen (PCNA)–positive cells, apoptotic cells, and tumor microvessels in immunohistologic studies were evaluated by the Student *t* test. A *P* value less than .05 was considered statistically significant.

Results

IL-23R expression in pediatric B-ALL cells and normal counterparts

IL-23R expression was investigated in 29 pediatric B-ALL cell samples and in their normal counterparts (n = 12). Figure 1A (top panels) shows IL-23R expression in pro-B ALL cells (mean percentage $IL\text{-}23R^+$ cells = 70%, range 48%-90%), early pre-B ALL cells (mean percentage $IL\text{-}23R^+$ cells = 66.3%, range 54%-82%), and pre-B ALL cells (mean percentage $IL\text{-}23R^+$ cells = 64%, range 35%-97%). Four-color staining of normal BM mononuclear cells for CD19, CD10, CD20, and IL-23R showed a mean percentage of 1.2% $IL\text{-}23R^+$ normal pro-B lymphocytes, 2.6% $IL\text{-}23R^+$ early pre-B cells, and 3.8% $IL\text{-}23R^+$ pre-B cells (Figure 1B). Quantitative PCR analysis of IL-23R mRNA in B-ALL samples (n = 29) and normal counterparts (n = 4) revealed that IL-23R transcript was up-regulated in neoplastic cells

Downloaded from http://ashpublications.net/blood/article-pdf/116/19/3887/1490759/zh804510003887.pdf by guest on 02 June 2024

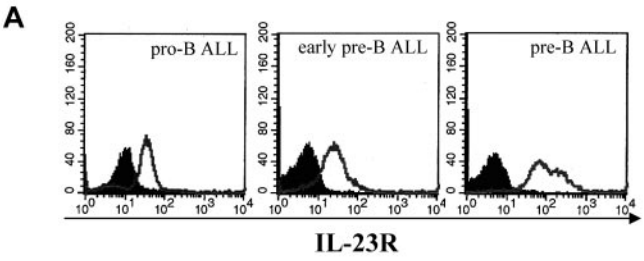

B

Normal early B cell samples	Pro-B	Early pre-B	Pre-B
# 1	5.1 %	4.3 %	48.5 %
# 2	1.4 %	1 %	3.5 %
# 3	7.8 %	9.5 %	3.4 %
# 4	1.7 %	8.8 %	3 %
# 5	0.5 %	2.6 %	3.3 %
# 6	0.8 %	2.5 %	22.5 %
# 7	35.7 %	0 %	4 %
# 8	0.9 %	1.4 %	6.8 %
# 9	0.2 %	0 %	0 %
# 10	3 %	45.7 %	29.5 %
# 11	0.7 %	1.9 %	17 %
# 12	0.5 %	5.3 %	3 %
Median	1.2 %	2.6 %	3.8 %

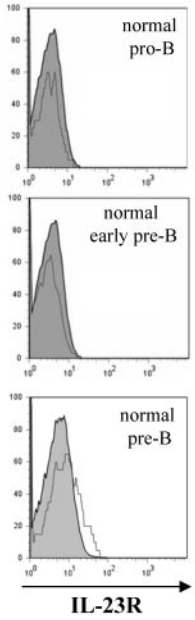

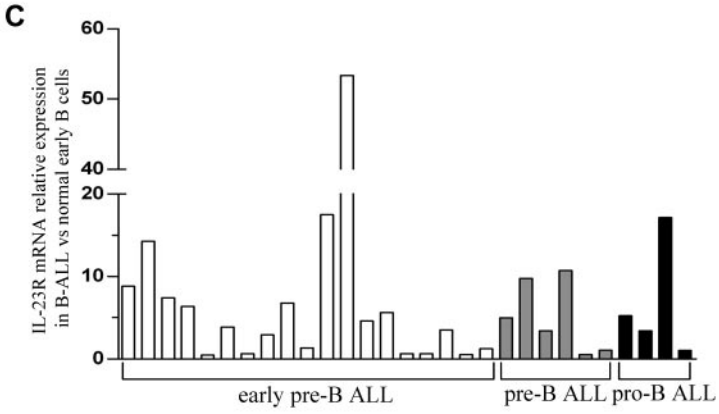

Figure 1. IL-23R expression in pediatric B-ALL cells and their normal counterparts. (A) IL-23R surface expression in B-ALL cells from BM patients, as assessed by flow cytometry. Open profile: IL-23R staining; dark profile: isotype matched mAb staining. (B) IL-23R expression on normal early B cells from 12 healthy individuals, by flow cytometry. Left panel: percentage of IL-23R expression in each cell sample. Histograms on the right: IL-23R staining in one representative normal pro-B (top panel), early pre-B (middle panel), and pre-B sample (bottom panel) is shown. Open profile: IL-23R staining; dark profile: isotype-matched mAb staining. (C) Relative quantification of IL-23R mRNA in 29 primary B-ALL samples, compared with their normal counterparts, by real-time PCR. Histograms represent fold differences of IL-23R expression between B-ALL and normal early B cells. The copy number of IL-23R mRNA was normalized on the endogenous reference (*GAPDH* gene) and expressed relative to a calibrator sample (mean value of 4 normal early B-cell samples) using the $2^{-(\Delta\Delta Ct)} \pm$ SD method.

(Figure 1C). Due to the paucity of IL-23R expressing early normal B lymphocytes, we investigated the functional activity of IL-23R in neoplastic B cells only.

IL-23 induces apoptosis and inhibits proliferation of primary B-ALL cells

Five different B-ALL cell suspensions (patients 2, 3, and 16 early pre-B ALL; patients 20 and 23 pre-B ALL) were cultured 24 and 48 hours with or without IL-23 at different concentrations (range 10-200 ng/mL) and tested for proliferation and apoptosis. At both time points, B-ALL cell proliferation was significantly inhibited at 100 ng/mL (Figure 2A) or 200 ng/mL (not shown) IL-23. The percentage of apoptotic cells was significantly increased by 100 ng/mL IL-23 treatment (Figure 2B) at 24 and 48 hours. These apoptotic cells were mostly annexin V/propidium iodide (PI) double-positive. Six-hour treatment with IL-23 or concentrations lower than 100 ng/mL did not affect apoptosis or proliferation in primary B-ALL cells (not shown). IL-23 did not affect the angiogenic potential of primary B-ALL cells, as assessed by CAM assay (IL-23, mean number of vessels = 21.6 ± 4; medium, mean number of vessels = 24.6 ± 3; data not shown).

IL-23 modulates miR expression in pediatric B-ALL cells

MiRs regulate tumor cell proliferation and apoptosis.[24-31] Thus, we investigated the ability of IL-23 to modulate miR expression in primary B-ALL cells. To this end, 6 B-ALL samples (patients 2, 3, 11, and 12 early pre-B ALL; patients 16 and 22 pre-B ALL) were cultured 24 hours with or without IL-23 and tested by human cancer miRNA PCR array, that allows detection of 84 different mature miRs implicated

Downloaded from http://ashpublications.net/blood/article-pdf/116/19/3887/1490759/zh804510003887.pdf by guest on 02 June 2024

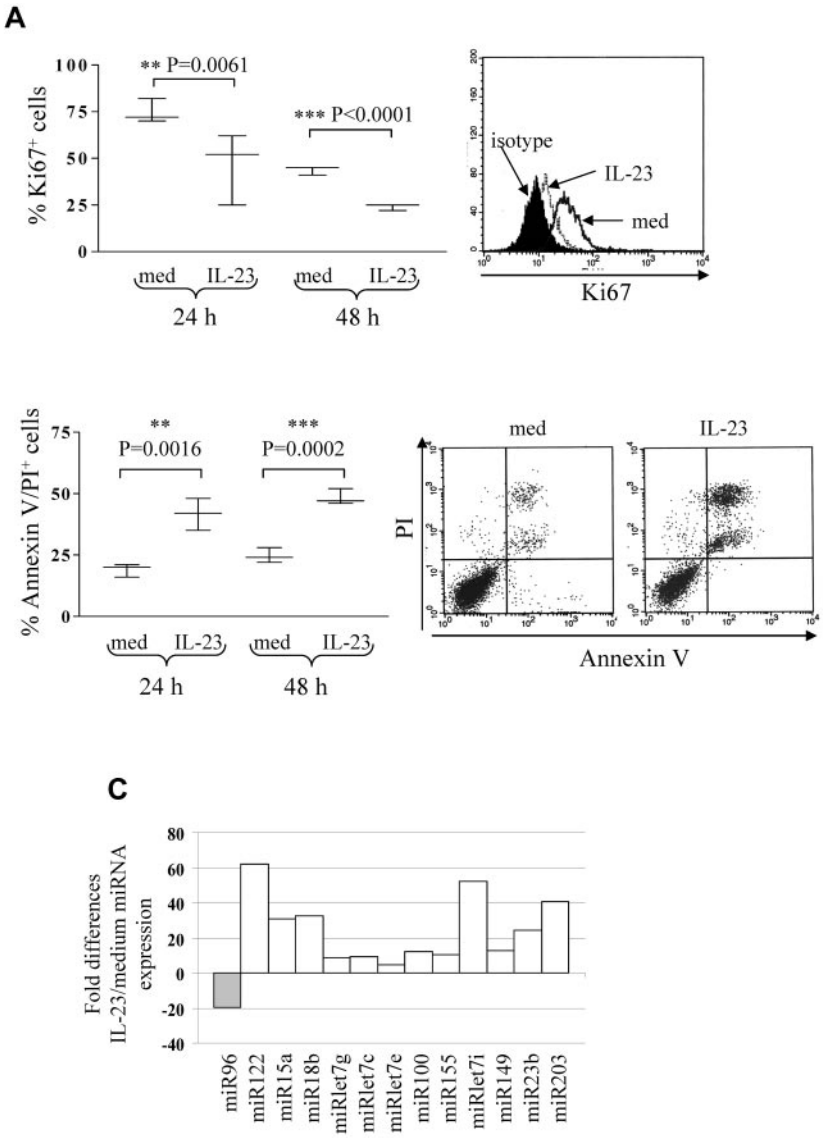

Figure 2. IL-23 activity on pediatric B-ALL cell proliferation and apoptosis. (A) Flow cytometric analysis of proliferating cells in primary B-ALL cells cultured 24 or 48 hours with or without IL-23. Left panel: whisker lines represent highest and lowest values, horizontal lines represent median values. One representative staining is shown in the right panel. Open profile: Ki67 staining in B-ALL cells cultured in medium alone (med); dashed profile: Ki67 staining in B-ALL cells treated with IL-23; dark profile: isotype-matched mAb staining in B-ALL cells treated with IL-23. (B) Flow cytometric analysis of apoptotic (annexin V^+/PI^+) cells in primary B-ALL cells cultured 24 or 48 hours with or without IL-23. Results represent the mean percentage of annexin V/PI–positive cells ± SD from 5 samples. One representative experiment is shown in the right panel. (C) MiRNA expression profile of 6 pooled primary B-ALL samples cultured with or without IL-23. Histograms represent fold differences of individual miRNA (miR) expression between B-ALL cells cultured with and without IL-23.

in tumorigenesis. Figure 2C shows the pooled results from the 6 B-ALL samples analyzed. IL-23 treatment down-regulated miR96 and up-regulated miR122, 15a, 18b, let7g, let7c, let7e, 100, 155, let7i, 149, 23b, and 203. Some of these up-regulated miRs (ie, let7 family members and miR15a) function as a tumor suppressor in different malignancies.[28,31,39] Analysis of single miR in each primary B-ALL sample revealed that miR15a only was consistently up-regulated in all samples, whereas all the other miR were regulated by IL-23 in 4 or 5 of the 6 samples.

IL-23 induces apoptosis of pediatric B-ALL cells through up-regulation of miR15a and consequent BCL-2 down-regulation

We next focused on the functional role of miR15a in B-ALL cells. MiR15a is involved in the control of apoptosis, since one of its targets is BCL-2.[39] Therefore, 5 B-ALL samples (patients 15-19) of the 6 tested for miR expression were cultured 48 hours with or without IL-23 and tested for BCL-2 expression. Figure 3A shows that, consistently with previous results,[40,41] BCL-2 was expressed in B-ALL cells and that IL-23 reduced significantly ($P = .0017$) BCL-2 expression. In order to establish a cause-and-effect link between IL-23 stimulation, miR15a up-regulation, BCL-2 down-regulation, and induction of apoptosis, the same B-ALL samples were transfected with anti-miR15a and treated with IL-23. After 48 hours, cells were tested for BCL-2 expression, by flow cytometry. These experiments demonstrated that primary B-ALL cells treated with IL-23 and transfected with anti-miR15a showed significantly ($P = .0034$) higher BCL-2 expression, compared with cells treated with IL-23 only or treated with IL-23 and transfected with irrelevant anti-miR (Figure 3A). The same B-ALL samples untransfected or transfected with irrelevant anti-miR and cultured with medium alone did not differ significantly in terms of BCL-2 expression (data not shown). Finally, 3 of the 5 samples tested in the above experiments were tested for apoptosis. As shown in Figure 3B, IL-23 alone induced apoptosis of primary B-ALL cells ($P = .0248$) whereas inhibition of miR15a caused a significant reduction ($P = .032$) of apoptotic cell number at basal level (cells cultured with medium alone). Transfection of primary B-ALL cells with irrelevant anti-miR did not affect apoptosis driven by IL-23. The same cell samples cultured with medium and transfected with irrelevant anti-miR did not differ significantly in terms of number of apoptotic cells (not shown).

To assess whether alternative apoptosis pathways should be involved in IL-23-driven apoptosis, we cultured 2 primary B-ALL

Downloaded from http://ashpublications.net/blood/article-pdf/116/19/3887/1490759/zh804510003887.pdf by guest on 02 June 2024

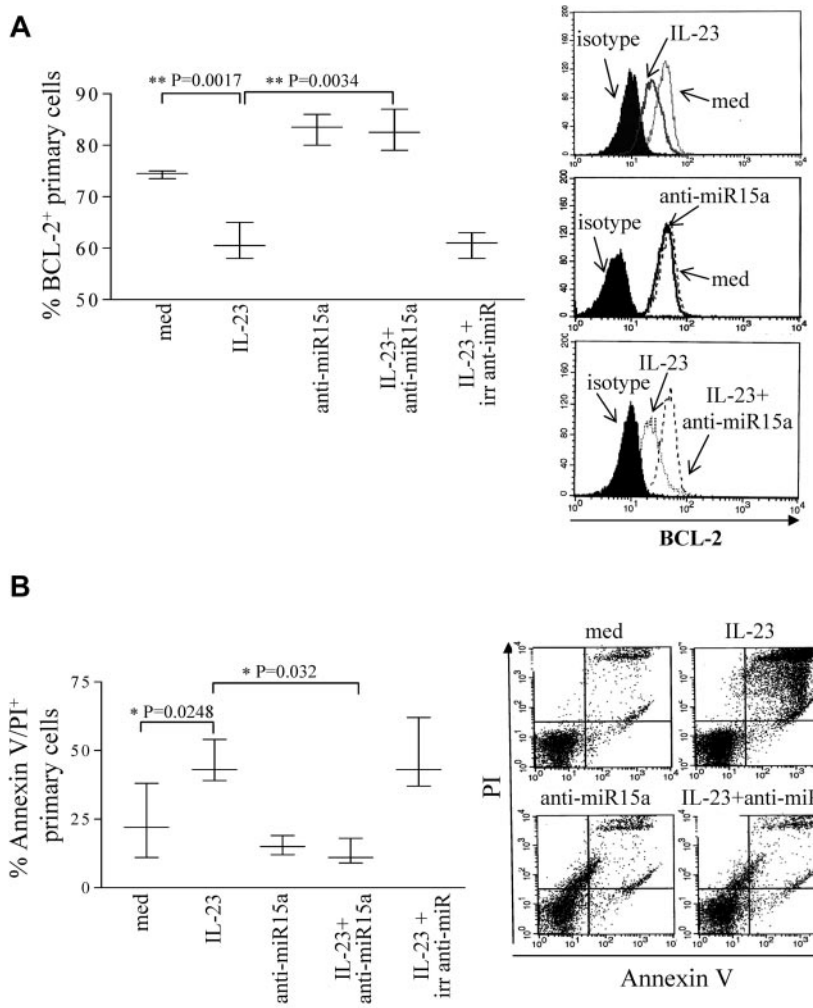

Figure 3. IL-23 driven apoptosis and BCL-2 modulation in pediatric B-ALL cells. (A) Left panel: flow cytometric analysis of BCL-2 expression in 5 B-ALL samples transfected or not with anti-miR15a or irrelevant (irr) anti-miR cultured 48 hours with or without IL-23. Left panel: whisker lines represent highest and lowest values, horizontal lines represent median values. Histograms on the right: BCL-2 intracellular staining of one representative experiment is shown. (B) Left panel: analysis of apoptotic cells in 3 B-ALL samples transfected or not with anti-miR15a or irrelevant anti-miR cultured 48 hours with or without IL-23. Left panel: whisker lines represent highest and lowest values, horizontal lines represent median values. Dot plots on the right: annexin V/PI double staining in 1 representative experiment.

samples with or without IL-23 for 30 minutes and 24 or 48 hours. Cells were subsequently analyzed for AKT or ERK1/2 phosphorylation (30 minutes of incubation) and activation of caspase-3, -7, -8, and -10 (24-48 hours), by flow cytometry. All these experiments gave negative results (not shown).

In vitro IL-23 antitumor activity against B-ALL cell lines

IL-23R was expressed in RS4;11 (18%), Nalm-6 (20%), and 697 (32%) cells, as assessed by flow cytometry (Figure 4A). The activity of IL-23 on 697 cells was tested in terms of (1) induction of signal transduction through the STAT pathway,[2] (2) modulation of cell proliferation and cell cycle, (3) induction of apoptosis and pathways involved, and (4) angiogenesis.

Unphosphorylated STAT1, 3, 5, and 6 were constitutively expressed in the 697 cells. STAT3 phosphorylation in serine 727 and tyrosine 705 residues was detected after IL-23 or IFN-α incubation. STAT1 or 5 phosphorylation was not induced by IL-23, but upon IFN-α incubation (Figure 4B). Phosphorylated STAT6 was expressed constitutively and not up-regulated by IL-23 or IFN-α. Constitutive STAT4 phosphorylation was visible in 697 cells and not increased by IL-23 or IFN-α, as assessed by Western blot (Figure 4B) and flow cytometry (Figure 4C).

IL-23 (100 ng/mL, but not lower concentrations) inhibited cell proliferation by 9 ± 2% (Ki67 staining, not shown) and reduced the percentage of cells in the G_2/M (mean percentage medium vs IL-23 treatment: 11% vs 6%) and G_0/G_1 phases (mean percentage medium vs IL-23 treatment: 36% vs 28%; Figure 4D). Furthermore, IL-23 induced apoptosis by 13% in the 697 cells (Figure 4D). Mitogens, including antihuman CD40, CpG2395, and antihuman Ig, did not affect significantly the 697-cell proliferation or cell cycle (not shown).

Similarly to primary B-ALL cells, IL-23 up-regulated miR15a (Figure 5A) and induced apoptosis (Figure 5B) in the 697 cells, through down-regulation of BCL-2 expression (Figure 5C-D). Silencing of miR15a (Figure 5A-D) or of IL-23R (not shown) abolished such effects in the 697 cells. Transfection with irrelevant anti-miR did not affect the ability of IL-23 to induce apoptosis (Figure 5B) and to reduce BCL-2 expression (Figure 5C). Alternative apoptosis pathways by IL-23 were investigated, including caspase activation, AKT or ERK1/2 or p38MAPK phosphorylation, and PARP cleavage. Figure 5E shows that IL-23 did not induce the activation of caspase-3, -7, -8, and -10 or phosphorylation of AKT, ERK1/2, and p38MAPK in the 697 cells. In addition, the Z-VAD-FMK pancaspase inhibitor did not affect the apoptosis driven by IL-23 (Figure 5F). By contrast, IL-23 induced PARP cleavage in the 697 cells, as assessed by flow cytometry and Western blot (Figure 5G). Taken together, these results demonstrated that the IL-23-driven apoptosis in the 697 cells was dependent on BCL-2 down-regulation and PARP cleavage, but not by caspase activation.

Finally, IL-23 did not change the angiogenic potential of the 697 cells (mean number of vessels IL-23 = 20 ± 3, medium = 24 ± 2, not shown).

Downloaded from http://ashpublications.net/blood/article-pdf/116/19/3887/1490759/zh804510003887.pdf by guest on 02 June 2024

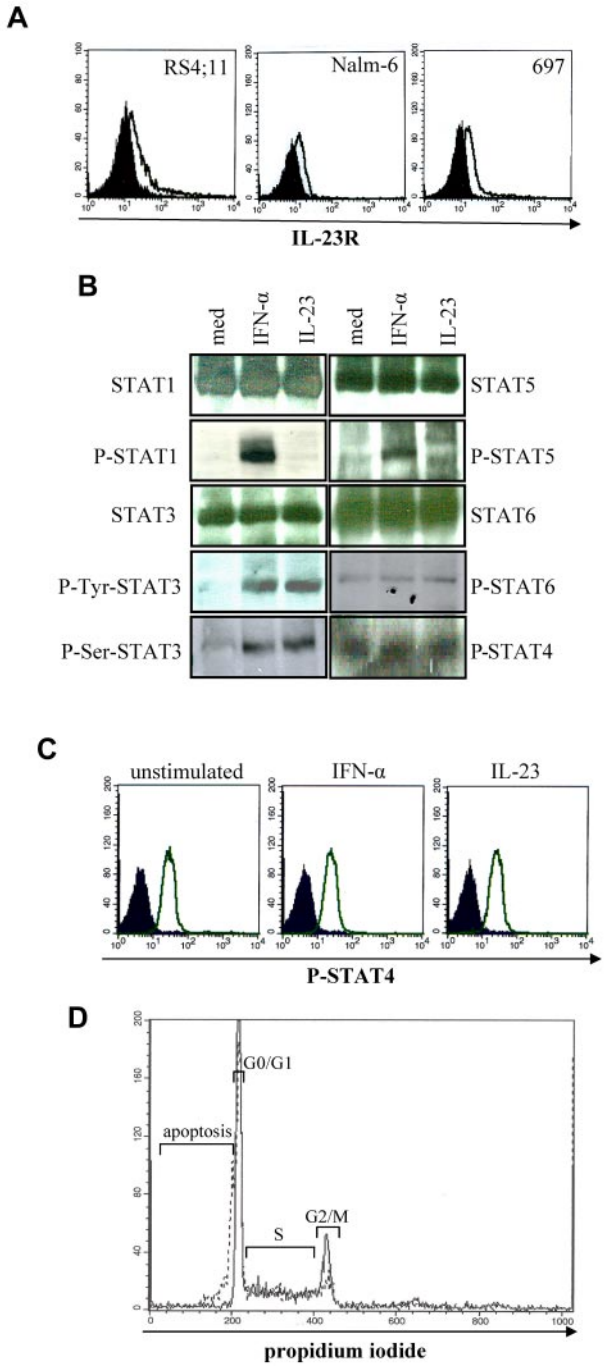

Figure 4. Expression of IL-23R and activity of IL-23 in B-ALL cell lines. (A) IL-23R surface expression in human B-ALL cell lines as assessed by flow cytometry. Open profile: IL-23R staining; dark profile: isotype-matched mAb staining. (B-C) Analysis of STAT pathway in 697 cells stimulated 30 minutes with IL-23 or of IFN-α (positive control), as assessed by Western blot (B) and flow cytometry (C). (D) Flow cytometric analysis of cell cycle in 697 cells cultured 48 hours with or without IL-23. Unbroken profile: 697 cells cultured with medium alone; dashed profile: 697 cells cultured in the presence of IL-23.

hrIL-23 strongly inhibits tumorigenicity of the 697 B-ALL cells in SCID/NOD mice

Since the 697 cells were previously shown to be tumorigenic upon intravenous injection into SCID/NOD mice,[42] they were selected for further studies. The 697 cell line was a suitable model for in vivo studies, because it shows functional similarities to the primary B-ALL cells (see above). Thus, 2 groups of 10 animals each were injected intravenously with 5×10^6 697 cells, treated with hrIL-23 or PBS (controls) intravenously, and killed after 14 days. Under these conditions, 697 cells give rise to bulky abdominal tumor masses.[42] Mice treated with hrIL-23 developed tumors significantly smaller ($P = .0001$) than mice receiving PBS (n = 10 for both groups; IL-23 treated, mean volume 24.8 mm^3; range 18.2-29 mm^3; controls, mean volume 40.8 mm^3; range 29-53 mm^3; Figure 6A). The abdominal tumor masses in PBS-treated mice consisted of proliferating lymphoblastoid cells (Figure 6B top left). Tumors from hrIL-23–treated mice showed more frequent apoptotic figures (Figure 6B top right), as confirmed by TUNEL assay (apoptotic indexes: controls, 7.5% ± 3.0% vs IL-23–treated mice, 15.2% ± 3.9%; $P < .005$), and a lower proliferation index, as revealed by PCNA immunostaining (proliferation indexes: controls, 91.4% ± 5.8% vs IL-23–treated mice, 70.3% ± 7.6%; $P < .005$; Figure 6B second row). Microvessel counts, as assessed by anti-CD31 immunostaining, were similar in tumors from PBS- and hrIL-23–treated mice (controls, 6.9 ± 2.2; hrIL-23–treated mice, 6.1 ± 1.8; Figure 6B third row). Tumors from controls displayed a distinct expression of cyclin D1 (Figure 6B bottom left), whereas such expression was strongly reduced in tumors from hrIL-23–treated mice (Figure 6B bottom right). Tumor infiltration with host mononuclear or polymorphonuclear cells was virtually undetectable in hrIL-23– and PBS-treated animals (not shown).

We next investigated, by PCR array, the expression of mature miR in tumors from hrIL-23– versus PBS-treated animals. In 2 different experiments performed with superimposable results, the expression of the following miRs were up-regulated by IL-23 (Figure 6C): miR222, 92a, 181a, 15a, 138, 29b, 29a, let7f, 181b, 34a, 27a, 372, and 181c. Conversely, miR10b and 32 were found to be down-regulated in tumors from hrIL-23– versus PBS-treated animals.

MiR15a knockdown abolishes the IL-23 antitumor activity in vivo

Next, the 697 cells were silenced for miR15a expression and tested for tumorigenicity in SCID/NOD mice upon hrIL-23 and PBS treatment. The 697 cells transfected with irrelevant anti-miR were used as controls. The experimental design was the following: 1 group of 5 animals was injected intravenously with 5×10^6 697 cells and treated with PBS; 1 group (n = 5) was injected with 5×10^6 697 cells and treated with hrIL-23; 1 group (n = 5) was injected with 5×10^6 697 cells transfected with anti-miR15a and treated with PBS; 1 group (n = 5) was injected with the latter cells and treated with hrIL-23; and the last group (n = 5) was injected with 5×10^6 697 cells transfected with irrelevant anti-miR and treated with hrIL-23. These experiments, repeated twice with similar results, demonstrated unambiguously that miR15a is necessary for IL-23 antitumor activity in vivo, since, according to our in vitro results, transfection with miR15a inhibitor, but not with irrelevant anti-miR, abolished the reduction of tumor growth driven by IL-23 (Figure 7A left panel). Quantitative PCR of miR15a expression from explanted tumors showed that IL-23 treatment up-regulated in vivo miR15a in wild-type 697 cells and in 697 cells transfected with irrelevant anti-miR, but not in 697 cells transfected with anti-miR15a (Figure 7A right panel).

MiR15a overexpression reduces the Nalm-6 cell spreading and cell growth of the 697 cell line in vivo

To investigate whether forced expression of miR15a had similar antitumor activity to hrIL-23 treatment in vivo, Nalm-6 cells

Downloaded from http://ashpublications.net/blood/article-pdf/116/19/3887/1490759/zh804510003887.pdf by guest on 02 June 2024

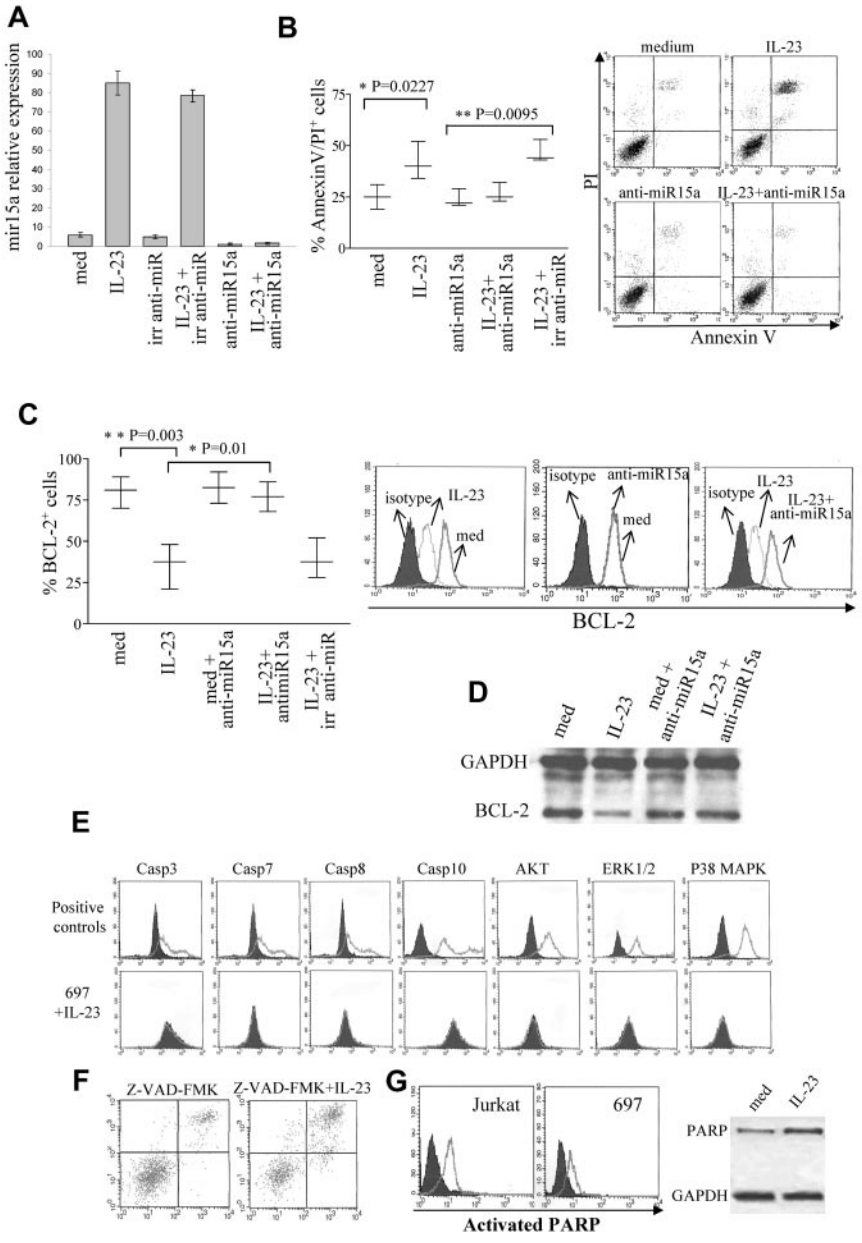

Figure 5. Apoptosis pathway driven by IL-23 in 697 cells. (A) Relative quantification of miR15a in wild-type 697 cells and 697 cells transfected with anti-miR15a or irrelevant (irr) anti-miR cultured 48 hours with or without IL-23, as assessed by real-time PCR. MiR15a expression was normalized to an endogenous reference (miRU6) and expressed relative to a calibrator sample (primary B-ALL sample). (B) Left panel: flow cytometric analysis of apoptosis in wild-type 697 and in 697 cells transfected with anti-miR15a or irrelevant anti-miR cultured 48 hours with or without IL-23 (med). Whisker lines represent highest and lowest values, horizontal lines represent median values (n = 3). Dot plots on the right: annexin V/PI double staining in one representative experiment is shown. (C) Left panel: flow cytometric analysis of BCL-2 expression in wild-type 697 cells and 697 cells transfected with anti-miR15a or irrelevant (irr) anti-miR cultured with medium (med) or IL-23 (48 hours). Whisker lines represent highest and lowest values; horizontal lines represent median values (n = 3). Histograms on the right: one representative experiment of BCL-2 staining is shown. (D) Western blot of BCL-2 expression in wild-type 697 cells and 697 cells transfected with anti-miR15a or irrelevant (irr) anti-miR upon incubation with medium (med) or IL-23 (48 hours). (E) Flow cytometric analysis of caspase activation and AKT, ERK/1, and p38MAPK phosphorylation in 697 cells upon incubation for 48 hours with medium or IL-23 (bottom panels). Positive controls are shown in top panels. Open profile: caspase-3, -7, -8, and -10, and phosphorylated AKT, ERK1/2, and p38MAPK staining in stimulated cells; dark profile: caspase-3, -7, -8, and -10 and phosphorylated AKT, ERK1/2, and p38MAPK staining in untreated cells. (F) Flow cytometric analysis of apoptosis of 697 cells pretreated 1 hour with the Z-VAD-FMK pancaspase inhibitor and then cultured for an additional 48 hours with medium (Z-VAD-FMK) or with IL-23 (Z-VAD-FMK+IL23). One representative experiment is shown. (G) PARP cleavage in 697 cells cultured 48 hours with medium (med) or with IL-23, as assessed by flow cytometry (histograms on the left) and by Western blot (right panel). Histogram plots: staining with anti-cleaved PARP Ab of cells cultured with IL-23 (open profile) or with medium (dark profile). Jurkat cells treated 5 hours with etoposide represent the positive control.

transfected with pEP-hsa-miR15a and the 697 cells transfected with hsa-miR15a precursor were tested for their tumorigenicity in SCID/NOD mice. Nalm-6 cells transfected with pEP-miR-null vector and 697 cells transfected with irrelevant miR precursor were used as controls. Quantitative PCR showed that (1) pEP-hsa-miR15a transfectants overexpressed miR15a, compared with pEP-miR-null transfectants or wild-type cells, and (2) miR15a 697 transfectants overexpressed miR15a, compared with irrelevant miR precursor transfectants or wild-type 697 cells (Figure 7B). Two groups of 5 animals each were injected intravenously with 5×10^6 wild-type Nalm-6 cells and treated with hrIL-23 or PBS. Two additional groups of 5 mice each were injected intravenously with 5×10^6 pEP-hsa-miR15a or pEP-miR-null vector cells. No tumor masses were grown, thus we searched leukemic cells in the peripheral blood (PB), spleens, and BM from each animal using the human CD10 and CD19 markers (expressed by wild-type Nalm-6 cells) and flow cytometric analysis. As shown in Figure 7C (top panels), $CD10^+CD19^+$ Nalm-6 cells were found in the PB (mean 22%), BM (mean 48%), and at low percentage in the spleens (mean 1.4%) of PBS-treated mice. IL-23 reduced the presence of Nalm-6 in the PB (mean 2.4%) and their spreading into the spleens (mean 0.4%) and BM (mean 14%; Figure 7C middle panels). Nalm-6 cells overexpressing miR15a were undetectable in the PB (mean 0.36%), spleens (mean 0.14%), and BM (mean $< 0.05\%$; Figure 7C bottom panels). PeP–miR-null transfected Nalm-6 cells were found in PB, spleen, and BM at similar percentages to wild-type Nalm-6 cells (not shown).

Accordingly, enforced expression of miR15a in the 697 cells caused a significant reduction of tumor cell growth in vivo (Figure 7A) compared with the wild-type 697 cells or to cells transfected with irrelevant miR. Finally, the volume of tumors from IL-23–treated mice injected with the wild-type 697 cells was similar to those formed in PBS-treated mice injected with the 697 cells overexpressing miR15a (Figure 7A).

Downloaded from http://ashpublications.net/blood/article-pdf/116/19/3887/1490759/zh804510003887.pdf by guest on 02 June 2024

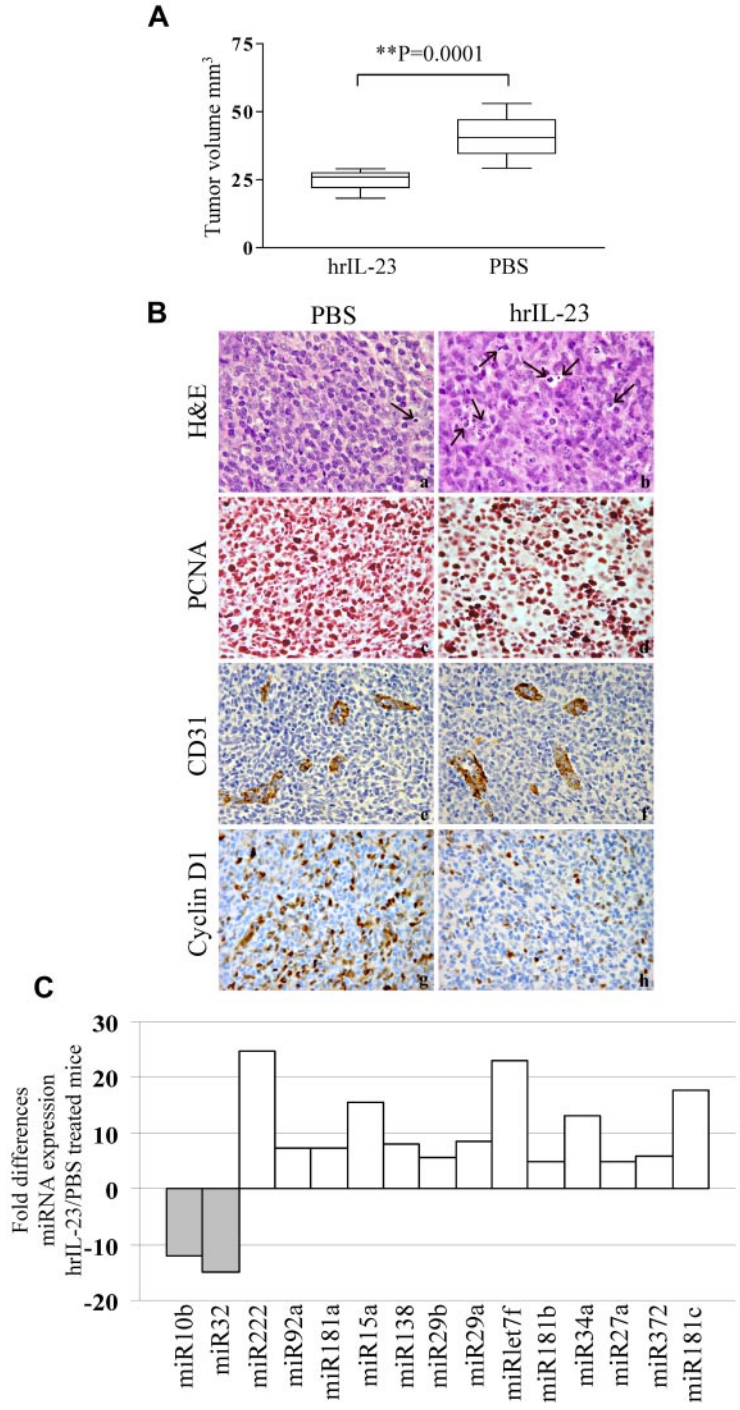

Figure 6. In vivo antitumor activity of IL-23. (A) Volume of tumors grown in PBS and hrIL-23–treated SCID/NOD mice 14 days after 697 cell intravenous inoculation. The differences in size between tumors removed from PBS- and hrIL-23–treated mice were evaluated by the Mann-Whitney U test. Boxes indicate values between the 25th and 75th percentiles, and whisker lines represent highest and lowest values for each group. Horizontal lines represent median values. (B) Morphologic and immunohistochemical analyses of tumors developed in PBS- and hrIL-23–treated mice after 697 cell intravenous inoculation. Arrows in top 2 images indicate apoptotic figures, as revealed by the aspect of chromatin condensation, cell shrinkage, and scattered apoptotic bodies. Anti-PCNA (images in second row), anti-CD31 (images in third row), and anti-cyclinD1 (images in fourth row) immunostaining results are shown. H&E and PCNA staining: magnification ×600 field (60× objective and 10× ocular lens; 0.120 mm^2 per field), CD31, and cyclin D1 staining: magnification ×400 field (40× objective and 10× ocular lens; 0.180 mm^2 per field. (C) miRNA gene expression profile in tumors explanted from hrIL-23– vs PBS-treated animals 14 days after 697 tumor cell inoculation. Histograms represent fold differences of individual miR expression between tumors formed in hrIL-23– vs PBS-treated animals.

Discussion

IL-23 belongs to a cytokine superfamily, including IL-12, that exerts direct antitumor activity in hematologic and nonhematologic malignancies.[37,38,42,43] In this study, we addressed the question of whether IL-23 could target pediatric B-ALL cells and inhibit directly their growth. The IL-12Rβ1 chain, shared by IL-12R and IL-23 receptor, was expressed in B-ALL cells and in their normal counterparts.[42] Here, we show that the other subunit of the IL-23 receptor, the IL-23R, was functional in primary B-ALL cells and strikingly up-regulated at the transcriptional level, compared with normal early B cells. We demonstrate that IL-23 damped directly B-ALL cell growth both in vitro and in vivo by inhibiting proliferation and inducing apoptosis through the modulation of miR15a and BCL-2. Tumorigenicity of B-ALL cell lines was studied in SCID/NOD mice to evaluate the antitumor activity of IL-23 in the absence of immune responses. Human IL-23 is active also on murine cells,[2] but the following findings support the conclusion that, in our model, the cytokine targeted directly human leukemic cells: (1) the in vivo antitumor mechanisms operated by IL-23 were overlapping with those detected in vitro, and (2) tumor

Downloaded from http://ashpublications.net/blood/article-pdf/116/19/3887/1490759/zh804510003887.pdf by guest on 02 June 2024

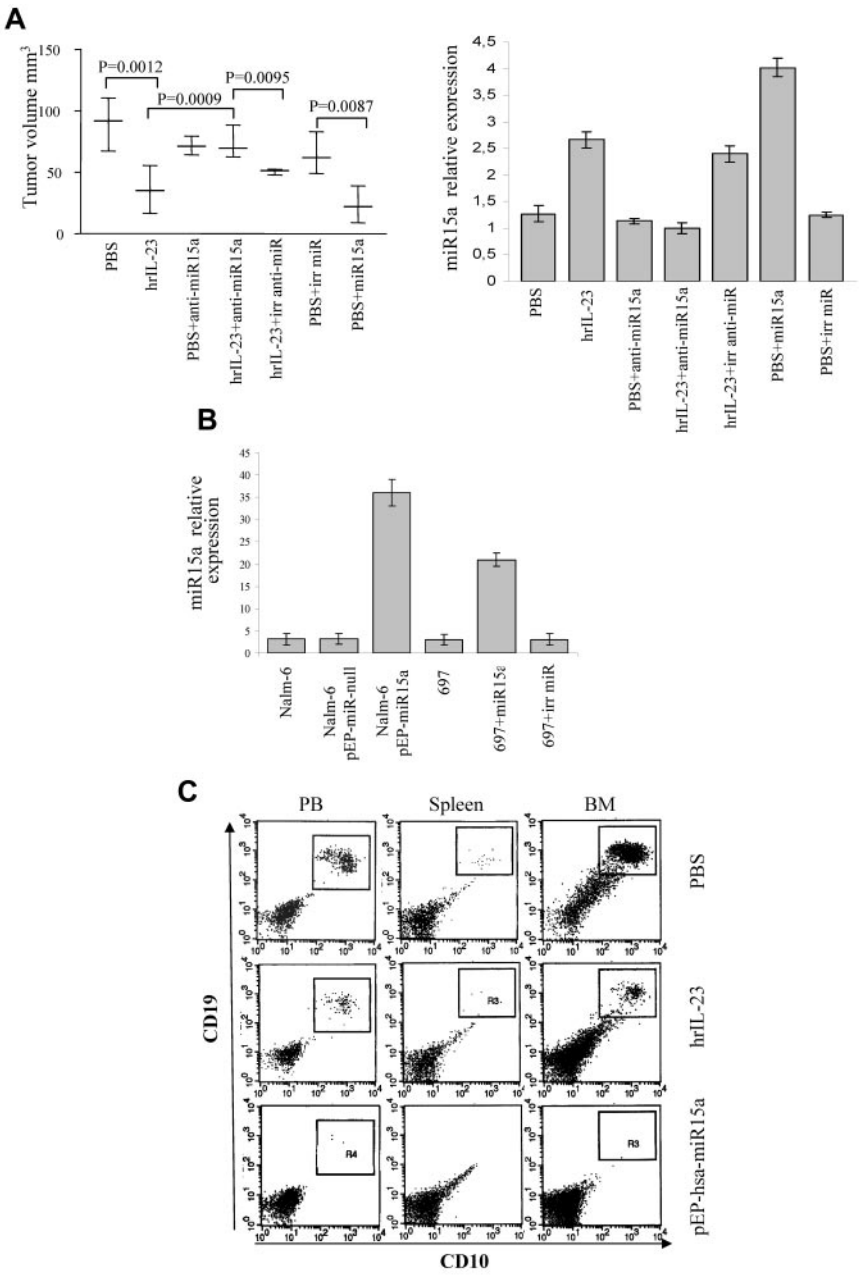

Figure 7. Effects of miR15a silencing and overexpression on tumorigenicity of B-ALL cells. (A) Left panel: volume of tumors grown in PBS- and hrIL-23–treated animals 14 days after intravenous injection of 697 cells transfected or not with anti-miR15a, irrelevant (irr) anti-miR, miR15a, or irrelevant pre-miR precursor (irr miR). Differences in tumors size were evaluated by the Mann-Whitney U test. Whisker lines represent highest and lowest values, horizontal lines represent median values. Right panel: relative quantification of miR15a expression in tumors explanted from PBS- or hrIL-23–treated animals injected with 697 cells transfected or not with anti-miR15a, irrelevant (irr) anti-miR, miR15a, or irrelevant pre-miR precursor. (B) Relative quantification of miR15a in wild-type and transfected Nalm-6 or 697 cells before injection. (C) Analysis of leukemic cell spreading in peripheral blood, spleen, and BM from hrIL-23– or PBS-treated mice injected intravenously with Nalm-6 cells transfected or not with pEP-has–-miR15a or pEP–miR-null (not shown). Analysis was performed 5 weeks after tumor cell inoculation. Nalm-6 cells were identified as human $CD10^+/CD19^+$ cells. One representative staining is shown.

infiltration with host mononuclear or polymorphonuclear cells was virtually undetectable. To gain more insight into the molecular mechanisms underlying the antitumor activity of IL-23, we investigated the modulation of mature miRNA expression induced by the cytokine both in vivo and in vitro. In this study, most miRNA modulated by IL-23 in primary B-ALL cells were different from miRNA regulated by the cytokine in tumors formed in vivo by the 697 cell line. These differences may depend on intrinsic characteristics of leukemic cells from patients versus the 697 cell line or the in vivo relationships established by the latter cells with the tumor microenvironment. The only miRNA up-regulated by IL-23 both in vitro and in vivo was miR15a; therefore, we focused on investigating whether up-regulation of miR15a was sufficient and necessary for IL-23 antitumor activity against leukemic cells. To this end, we analyzed the IL-23 effects on B-ALL cells in which miR15a was silenced. In addition, we investigated whether forced expression of miR15a had a similar antitumor activity to the treatment of IL-23. Taken together, these experiments allowed us to demonstrate that knockdown of miR15a rendered B-ALL cells unresponsive to IL-23 in vitro and in vivo, and that enforced expression of miR15a inhibited leukemic cell growth in vivo. Studies on the mechanisms underlying the proapoptotic effect of IL-23 showed that the cytokine down-regulated the antiapoptotic BCL-2 and induced PARP cleavage in the absence of caspase activation. Although PARP represents a main cleavage target of caspases,[44] alternative pathways may activate PARP as reported in T lymphocytes treated with methotrexate, lung cancer cells transduced for MBP-1, and breast cancer cells treated with PI3K/mTOR inhibitor.[45-48]

Here, we show that IL-23 exerted also antiproliferative effects on B-ALL cells that may be ascribed to 2 different mechanisms. First, we demonstrated that IL-23 treatment damped in vivo expression of cyclin D1, another target of miR15a,[49] whose functions are directly associated with cancer progression and invasion.[49,50] Second, IL-23 treatment induced up-regulation of

Downloaded from http://ashpublications.net/blood/article-pdf/116/19/3887/1490759/zh804510003887.pdf by guest on 02 June 2024

miR let7-g, -c, -e, and -i in primary B-ALL samples. The let-7 family miRNA negatively regulated the RAS family oncogenes, and inhibition of let-7g and -e caused growth acceleration of lung adenocarcinoma cells.[32] It is therefore conceivable that modulation of miRNA let-7g, -c, -e, and -i may be involved in the antiproliferative activity of IL-23 on B-ALL cells. We[42] have previously demonstrated that childhood B-ALL cells display methylation of a CpG island in the noncoding exon 1 of the IL-12RB2 gene. This epigenetic event prevents expression of the IL-12Rβ2 protein and, consequently, the assembly of the functional heterodimeric IL-12R. In other models,[38] we have shown that reexpression of the *IL-12RB2* gene, achieved by treating malignant cells with a demethylating agent, renders the latter cells sensitive to the antiproliferative and proapoptotic effects of IL-12. Transfer of these findings to the clinical setting is not an easy task. The results of this study delineate a completely different situation for IL-23R that is highly expressed in pediatric B-ALL cells and mediates IL-23-driven, direct inhibition of tumor growth. Therefore, in principle, IL-23 may be a good candidate drug to be tested in a phase I trial in childhood B-ALL patients otherwise unresponsive to current therapeutic standards. An additional argument in favor of this proposal is the low toxicity shown by IL-23 in animal models, likely in relation to the low induction of IFN-γ in vivo.[19]

Acknowledgments

This work was supported by grants from Associazione Italiana Ricerca sul Cancro, Milano, Italy (grant no: 4014 to I.A.), Fondazione Cassa di Risparmio della Provincia di Chieti (CariChieti), Italy (to E.D.C.), Fondazione Città Della Speranza, Fondazione CARIPARO, PRIN, and AIRC (to G.B.).

Authorship

Contribution: C.C., S.C., C.F., E.D.C., D.R., and I.P. performed research and analyzed data; E.O. and D.R. performed research; G.B. contributed patient samples; and I.A. designed research, analyzed data, and wrote the manuscript.

Conflict-of-interest disclosure: The authors declare no competing financial interests.

Correspondence: Irma Airoldi, AIRC Laboratory of Immunology and Tumors, Department of Experimental and Laboratory Medicine, G. Gaslini Institute, Largo G. Gaslini 5, 16148 Genova, Italy; e-mail: irmaairoldi@ospedale-gaslini.ge.it.

References

1. Oppmann B, Lesley R, Blom B, et al. Novel p19 protein engages IL-12p40 to form a cytokine, IL-23, with biological activities similar as well as distinct from IL-12. *Immunity.* 2000;13(5):715-725.
2. Parham C, Chirica M, Timans J, et al. A receptor for the heterodimeric cytokine IL-23 is composed of IL-12Rbeta1 and a novel cytokine receptor subunit, IL-23R. *J Immunol.* 2002;168(11):5699-5708.
3. Re F, Strominger JL. Toll-like receptor 2 (TLR2) and TLR4 differentially activate human dendritic cells. *J Biol Chem.* 2001;276(40):37692-37699.
4. Napolitani G, Rinaldi A, Bertoni F, Sallusto F, Lanzavecchia A. Selected Toll-like receptor agonist combinations synergistically trigger a T helper type 1-polarizing program in dendritic cells. *Nat Immunol.* 2005;6(8):769-776.
5. Carmody RJ, Ruan Q, Liou HC, Chen YH. Essential roles of c-Rel in TLR-induced IL-23 p19 gene expression in dendritic cells. *J Immunol.* 2007;178(1):186-191.
6. Verreck FA, de Boer T, Langenberg DM, et al. Human IL-23-producing type 1 macrophages promote but IL-10-producing type 2 macrophages subvert immunity to (myco)bacteria. *Proc Natl Acad Sci U S A.* 2004;101(13):4560-4565.
7. Cua DJ, Sherlock J, Chen Y, et al. Interleukin-23 rather than interleukin-12 is the critical cytokine for autoimmune inflammation of the brain. *Nature.* 2003;421(6924):744-748.
8. Hue S, Ahern P, Buonocore S, et al. Interleukin-23 drives innate and T cell-mediated intestinal inflammation. *J Exp Med.* 2006;203(11):2473-2483.
9. Kryczek I, Bruce AT, Gudjonsson JE, et al. Induction of IL-17+ T cell trafficking and development by IFN-gamma: mechanism and pathological relevance in psoriasis. *J Immunol.* 2008;181(7):4733-4741.
10. Caruso R, Pallone F, Monteleone G. Emerging role of IL-23/IL-17 axis in H pylori-associated pathology. *World J Gastroenterol.* 2007;13(42):5547-5551.
11. Langowski JL, Kastelein RA, Oft M. Swords into plowshares: IL-23 repurposes tumor immune surveillance. *Trends Immunol.* 2007;28(5):207-212.
12. Langowski JL, Zhang X, Wu L, et al. IL-23 promotes tumour incidence and growth. *Nature.* 2006;442(7101):461-465.
13. Lin WW, Karin M. A cytokine-mediated link between innate immunity, inflammation, and cancer. *J Clin Invest.* 2007;117(5):1175-1183.
14. Numasaki M, Watanabe M, Suzuki T, et al. IL-17 enhances the net angiogenic activity and in vivo growth of human non-small cell lung cancer in SCID mice through promoting CXCR-2-dependent angiogenesis. *J Immunol.* 2005;175(9):6177-6189.
15. Tartour E, Fossiez F, Joyeux I, et al. Interleukin 17, a T-cell–derived cytokine, promotes tumorigenicity of human cervical tumors in nude mice. *Cancer Res.* 1999;59(15):3698-3704.
16. Hu J, Yuan X, Belladonna ML, et al. Induction of potent antitumor immunity by intratumoral injection of interleukin 23–transduced dendritic cells. *Cancer Res.* 2006;66(17):8887-8896.
17. Kaiga T, Sato M, Kaneda H, Iwakura Y, Takayama T, Tahara H. Systemic administration of IL-23 induces potent antitumor immunity primarily mediated through Th1-type response in association with the endogenously expressed IL-12. *J Immunol.* 2007;178(12):7571-7580.
18. Lo CH, Lee SC, Wu PY, et al. Antitumor and antimetastatic activity of IL-23. *J Immunol.* 2003;171(2):600-607.
19. Oniki S, Nagai H, Horikawa T, et al. Interleukin-23 and interleukin-27 exert quite different antitumor and vaccine effects on poorly immunogenic melanoma. *Cancer Res.* 2006;66(12):6395-6404.
20. Overwijk WW, de Visser KE, Tirion FH, et al. Immunological and antitumor effects of IL-23 as a cancer vaccine adjuvant. *J Immunol.* 2006;176(9):5213-5222.
21. Shan BE, Hao JS, Li QX, Tagawa M. Antitumor activity and immune enhancement of murine interleukin-23 expressed in murine colon carcinoma cells. *Cell Mol Immunol.* 2006;3(1):47-52.
22. Ugai S, Shimozato O, Yu L, et al. Transduction of the IL-21 and IL-23 genes in human pancreatic carcinoma cells produces natural killer cell-dependent and -independent antitumor effects. *Cancer Gene Ther.* 2003;10(10):771-778.
23. Yuan X, Hu J, Belladonna ML, Black KL, Yu JS. Interleukin-23-expressing bone marrow–derived neural stem-like cells exhibit antitumor activity against intracranial glioma. *Cancer Res.* 2006;66(5):2630-2638.
24. Calin GA, Dumitru CD, Shimizu M, et al. Frequent deletions and down-regulation of micro-RNA genes miR15 and miR16 at 13q14 in chronic lymphocytic leukemia. *Proc Natl Acad Sci U S A.* 2002;99(24):15524-15529.
25. Calin GA, Liu CG, Sevignani C, et al. MicroRNA profiling reveals distinct signatures in B cell chronic lymphocytic leukemias. *Proc Natl Acad Sci U S A.* 2004;101(32):11755-11760.
26. Calin GA, Sevignani C, Dumitru CD, et al. Human microRNA genes are frequently located at fragile sites and genomic regions involved in cancers. *Proc Natl Acad Sci U S A.* 2004;101(9):2999-3004.
27. Eis PS, Tam W, Sun L, et al. Accumulation of miR-155 and BIC RNA in human B cell lymphomas. *Proc Natl Acad Sci U S A.* 2005;102(10):3627-3632.
28. Johnson SM, Grosshans H, Shingara J, et al. RAS is regulated by the let-7 microRNA family. *Cell.* 2005;120(5):635-647.
29. Metzler M, Wilda M, Busch K, Viehmann S, Borkhardt A. High expression of precursor microRNA-155/BIC RNA in children with Burkitt lymphoma. *Genes Chrom Cancer.* 2004;39(2):167-169.
30. Michael MZ, SM OC, van Holst Pellekaan NG, Young GP, James RJ. Reduced accumulation of specific microRNAs in colorectal neoplasia. *Mol Cancer Res.* 2003;1(12):882-891.
31. Takamizawa J, Konishi H, Yanagisawa K, et al. Reduced expression of the let-7 microRNAs in human lung cancers in association with shortened postoperative survival. *Cancer Res.* 2004;64(11):3753-3756.
32. Kumar MS, Lu J, Mercer KL, Golub TR, Jacks T. Impaired microRNA processing enhances cellular transformation and tumorigenesis. *Nat Genet.* 2007;39(5):673-677.
33. Lu J, Getz G, Miska EA, et al. MicroRNA expression profiles classify human cancers. *Nature.* 2005;435(7043):834-838.
34. Basso G, Buldini B, De Zen L, Orfao A. New methodologic approaches for immunophenotyping acute leukemias. *Haematologica.* 2001;86(7):675-692.

Downloaded from http://ashpublications.net/blood/article-pdf/116/19/3887/1490759/zh804510003887.pdf by guest on 02 June 2024

35. Airoldi I, Meazza R, Croce M, et al. Low-dose interferon-gamma-producing human neuroblastoma cells show reduced proliferation and delayed tumorigenicity. *Br J Cancer.* 2004;90(11): 2210-2218.
36. Ribatti D, Gualandris A, Bastaki M, et al. New model for the study of angiogenesis and antiangiogenesis in the chick embryo chorioallantoic membrane: the gelatin sponge/chorioallantoic membrane assay. *J Vasc Res.* 1997;34(6):455-463.
37. Airoldi I, Cocco C, Giuliani N, et al. Constitutive expression of IL-12R beta 2 on human multiple myeloma cells delineates a novel therapeutic target. *Blood.* 2008;112(3):750-759.
38. Airoldi I, Di Carlo E, Banelli B, et al. The IL-12Rbeta2 gene functions as a tumor suppressor in human B cell malignancies. *J Clin Invest.* 2004; 113(11):1651-1659.
39. Cimmino A, Calin GA, Fabbri M, et al. miR-15 and miR-16 induce apoptosis by targeting BCL2. *Proc Natl Acad Sci U S A.* 2005;102(39):13944-13949.
40. Laane E, Panaretakis T, Pokrovskaja K, et al. Dexamethasone-induced apoptosis in acute lymphoblastic leukemia involves differential regulation of Bcl-2 family members. *Haematologica.* 2007;92(11):1460-1469.
41. Wang L, Chen L, Benincosa J, Fortney J, Gibson LF. VEGF-induced phosphorylation of Bcl-2 influences B lineage leukemic cell response to apoptotic stimuli. *Leukemia.* 2005;19(3):344-353.
42. Airoldi I, Cocco C, Di Carlo E, et al. Methylation of the IL-12Rbeta2 gene as novel tumor escape mechanism for pediatric B-acute lymphoblastic leukemia cells. *Cancer Res.* 2006;66(8):3978-3980.
43. Airoldi I, Di Carlo E, Cocco C, et al. Endogenous IL-12 triggers an antiangiogenic program in melanoma cells. *Proc Natl Acad Sci U S A.* 2007; 104(10):3996-4001.
44. Tewari M, Quan LT, O'Rourke K, et al. Yama/CPP32 beta, a mammalian homolog of CED-3, is a CrmA-inhibitable protease that cleaves the death substrate poly(ADP-ribose) polymerase. *Cell.* 1995;81(5):801-809.
45. Ghosh AK, Steele R, Ryerse J, Ray RB. Tumor-suppressive effects of MBP-1 in non-small cell lung cancer cells. *Cancer Res.* 2006;66(24): 11907-11912.
46. Nielsen CH, Albertsen L, Bendtzen K, Baslund B. Methotrexate induces poly(ADP-ribose) polymerase-dependent, caspase 3-independent apoptosis in subsets of proliferating CD4+ T cells. *Clin Exp Immunol.* 2007;148(2):288-295.
47. Yu SW, Wang H, Poitras MF, et al. Mediation of poly(ADP-ribose) polymerase-1-dependent cell death by apoptosis-inducing factor. *Science.* 2002;297(5579):259-263.
48. Brachmann SM, Hofmann I, Schnell C, et al. Specific apoptosis induction by the dual PI3K/mTor inhibitor NVP-BEZ235 in HER2 amplified and PIK3CA mutant breast cancer cells. *Proc Natl Acad Sci U S A.* 2009;106(52):22299-22304.
49. Bonci D, Coppola V, Musumeci M, et al. The miR-15a-miR-16-1 cluster controls prostate cancer by targeting multiple oncogenic activities. *Nat Med.* 2008;14(11):1271-1277.
50. Sherr CJ. Cancer cell cycles. *Science.* 1996; 274(5293):1672-1677.

Downloaded from http://ashpublications.net/blood/article-pdf/116/19/3887/1490759/zh804510003887.pdf by guest on 02 June 2024